Available online at www.sciencedirect.com
ScienceDirect
Journal of the European Ceramic Society 31 (2011) 2775–2781
www.elsevier.com/locate/jeurceramsoc

Glass formation area and characterization studies in the $CdO–WO_3–TeO_2$ ternary system

A.E. Ersundu *, M. Çelikbilek, N. Solak, S. Aydin *

Istanbul Technical University, Department of Metallurgical and Materials Engineering, Istanbul 34469, Turkey

Received 26 April 2011; received in revised form 14 July 2011; accepted 23 July 2011
Available online 16 August 2011

Abstract

The glass formation area in the $CdO–WO_3–TeO_2$ ternary system was determined and thermal and structural features of the ternary glasses were characterized by differential scanning calorimetry (DSC), X-ray diffraction (XRD) and Raman scattering methods and the variation of the glass properties and structural transformations were discussed in terms of the glass composition comparing with the literature. For all ternary glass samples, the glass transition (T_g) and crystallization (T_c/T_p) temperatures, glass stability (ΔT), activation enthalpy for glass transition (ΔH^*) and fragility parameter (m) values were calculated from the DSC thermograms. Density (ρ), molar volume (V_M) and oxygen molar volume (V_O) values and the refractive indices (n) at a wavelength of 632 nm were measured. Raman spectra of the glasses were interpreted in terms of the structural transformations on the glass network resulted by the changing $WO_3 + CdO/TeO_2$ ratio.

Keywords: $CdO–WO_3–TeO_2$; Glass; Thermal properties; Spectroscopy

1. Introduction

Tellurite glasses have drawn considerable attention as promising candidates for optical fibers and non-linear optical devices on the account of their easy fabrication at low temperature, relatively low-phonon energy, high refractive index and dielectric constant, good infrared transmission, high thermal and chemical stability and low crystallization ability.[1–19] Furthermore, the structure of tellurite based glasses is also of interest, because there are two types of basic structural units, i.e. TeO_4 trigonal bipyramid (tbp) and TeO_3 trigonal pyramid (tp).[3,20]

It is known that pure tellurium oxide (TeO_2) does not have glass forming ability under normal quenching rates; therefore addition of network modifiers is needed to form tellurite-based glasses.[1,3,5–9] Addition of WO_3, as a network modifier or intermediate oxide network, to tellurite glasses provides advantageous properties, such as doping with rare-earth elements in a wide range, modifying the composition by a third, fourth, and even fifth component, enhancing the chemical stability and devitrification resistance.[1,2,5,9] Furthermore, tungsten–tellurite glasses have slightly higher phonon energy and higher glass transition temperature compared to other tellurite glasses; therefore they can be used at high optical intensities without exposure to thermal damage.[7–9,14,21] A considerable number of publications have been published on tungsten–tellurite glasses by different researchers because of its importance in optical applications.[1–19] Apart from this, previous studies on tellurite glasses containing CdO suggest that the addition of CdO enhances the optical properties.[22] CdO, as a network modifier, stabilizes the glass structure and improves the electrical properties by increasing the dielectric constant.[23]

First glasses in the $CdO–WO_3–TeO_2$ system were obtained by Imaoka and Yamazaki in their study on the glass formation range of various tellurite based binary and ternary systems.[24] Later, Safonov reported the glass formation range of this ternary system in his study on the liquidus surface projection of the $BaO(CdO)–WO_3–TeO_2$ ternary systems.[25] However, to the best of author's knowledge, the reported data available in the literature on the glass formation range is not detailed and there exist no information on the thermal and structural properties of the $CdO–WO_3–TeO_2$ ternary glasses.

In order to develop tellurite based glasses for optical applications, an understanding of their thermal and structural behavior is

* Corresponding authors. Tel.: +90 212 285 72 03; fax: +90 212 285 34 27.
E-mail addresses: ersundu@itu.edu.tr, ersundu@gmail.com (A.E. Ersundu), saydin@itu.edu.tr (S. Aydin).

0955-2219/$ – see front matter © 2011 Elsevier Ltd. All rights reserved.
doi:10.1016/j.jeurceramsoc.2011.07.027

crucial. Therefore, in the present study the authors aim to determine the glass formation area of the CdO–WO_3–TeO_2 ternary system and investigate the thermal and structural behavior of the CdO–WO_3–TeO_2 glasses by conducting detailed and systematical DSC, XRD and Raman analyses.

2. Experimental procedure

In the experimental studies, to determine the glass formation area, different compositions of the CdO–WO_3–TeO_2 system were prepared using a conventional melt-quenching technique. High purity powders of TeO_2 (99.99% purity, Alfa Aesar), WO_3 (99.8% purity, Alfa Aesar) and CdO (99.95% purity, Alfa Aesar) were thoroughly mixed and 5 g size powder batches were melted in a platinum crucible with a closed lid at 750–800 °C for 30 min in an electrical furnace and quenched in water bath.

The amorphous structure of the as-cast samples was checked by XRD analyses, which were carried out with powdered glass samples in a Bruker^{TM} D8 Advanced Series powder diffractometer using Cu K_α radiation in the 2θ range from 10° to 90°. After determining the glass formation area, all thermal and structural analyses were realized with the ternary glass samples. Original and final compositions of the samples are given in Table 1. The final compositions were calculated by performing chemical analysis using a Perkin Elmer AAnalyst 800 atomic absorption spectrometer with an error estimate of ±2%.

To recognize the thermal behavior of the glass samples, differential scanning calorimetry analyses were carried out in a Netzsch DSC 204 F1 (limit of detection: <0.1 μW, with an error estimate of ±1 °C) using a constant sample weight of 25 ± 1 mg in aluminum pans, under flowing (25 ml/min) argon gas with a heating rate of 10 °C/min. The glass transition (T_g), first crystallization onset and peak (T_c/T_p) temperatures were determined from the DSC thermograms. The glass transition temperatures (T_g) were taken as the inflection point of the endothermic change of the calorimetric signal. Crystallization onset temperatures were specified as the beginning of the reaction where the crystallization first starts and peak temperatures represent the maximum value of the exotherm. The temperature difference between the glass transition (T_g) and the first exothermic peak onset (T_c), $\Delta T = T_c - T_g$, indicating the value of glass stability was calculated.

The fragility parameter, m, of the glass samples was calculated (with an error estimate of ±1) from the following expression[26,27]:

$$m = \left(\frac{\Delta H^*}{RT_g}\right) \quad (1)$$

where m is the fragility parameter, ΔH^* is the activation enthalpy for glass transition, R is the gas constant and T_g is the glass transition temperature.

To determine the fragility parameter, m, the activation enthalpy for glass transition, ΔH^*, was calculated by running DSC scans of glass samples at four different heating rates, β

Table 1
Values of glass transition (T_g), first crystallization onset and peak (T_c/T_p), glass stability (ΔT), activation enthalpy for glass transition (ΔH^*), fragility parameter (m), refractive index (n), density (ρ), molar volume (V_M) and oxygen molar volume (V_O) of the ternary glass samples.

Sample ID	Original compositions (mol%)			Final compositions (mol%)			T_g (°C)	T_c/T_p (°C)	ΔT (°C)	ΔH^* (kJ mol^{-1})	m	n (at 632 nm)	ρ at 25 °C (g cm^{-3})	ρ theoretical (g cm^{-3})	V_M (cm^3 mol^{-1})	V_O (cm^3 mol^{-1})
	CdO	WO_3	TeO_2	CdO	WO_3	TeO_2										
CWT1	5	5	90	4.6	5.5	89.9	319	345/361	26	807	163	2.03	5.82	5.87	27.77	13.89
CWT2	10	5	85	9.2	5.2	85.6	325	346/347	21	815	151	2.11	5.85	5.99	27.37	14.03
CWT3	5	10	85	4.6	12.4	83.0	336	379/404	43	690	149	2.09	5.90	5.94	28.01	13.66
CWT4	10	10	80	9.1	10.2	80.7	339	365/366	26	669	131	2.14	5.88	6.01	27.84	13.92
CWT5	15	15	70	13.9	16.2	69.9	363	387/388	24	753	142	2.19	6.13	6.27	27.04	13.52
CWT6	10	20	70	8.9	22.3	68.8	366	429/438	63	505	142	2.17	6.06	6.21	28.20	13.43
CWT7	20	20	60	18.3	23.0	58.7	387	413/416	26	680	137	2.21	6.22	6.46	26.98	13.49

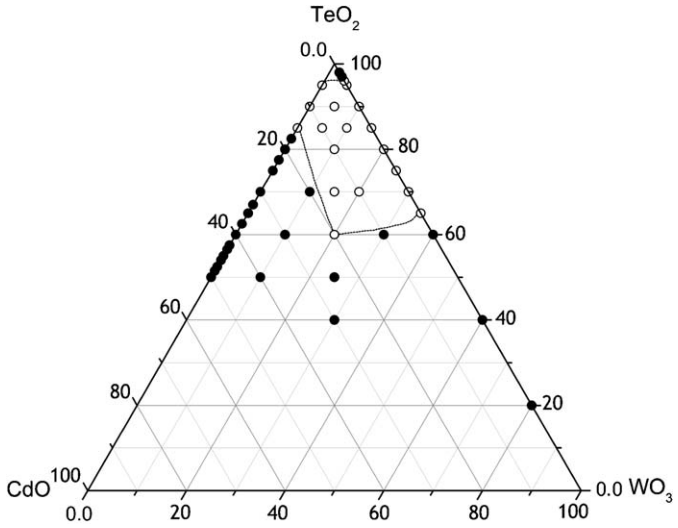

Fig. 1. Glass-formation area of the CdO–WO_3–TeO_2 ternary system: (◯) glass and (●) crystalline.

(5, 10, 15, 20 °C/min), and plotting the linear fits of ln β versus $1000/T_g$ according to the following expression[26,28]:

$$\ln \beta = \frac{-\Delta H^*}{RT_g} + \text{const} \quad (2)$$

where β is the heating rate, R is the gas constant and T_g is the glass transition temperature.

Densities, ρ, of the glasses were determined at room temperature by the Archimedes principle using distilled water as the immersion liquid and a digital balance of sensitivity 10^{-4} g. The density values obtained by repeated measurements showed an error of ±0.2%.

The molar volume, V_M, was calculated as a function of the molar fraction of each of the three components and the oxygen molar volume, V_O, was calculated by using the following expression[29]:

$$V_O = \left(\sum \frac{x_i M_i}{\rho}\right)\left(\frac{1}{\sum x_i n_i}\right) \quad (3)$$

where x_i is the molar fraction of each component i; M_i is the molecular weight; ρ is the glass density and n_i is the number of oxygen atoms in each oxide.

Refractive indices, n, at a wavelength of 632 nm were obtained at room temperature using a J.A. Woollam VASE and Gaertner L116C Ellipsometer. Glass samples were run at an incidence angle of 70°. The ellipsometer was calibrated using a silicon wafer standard before each run.

Raman scattering spectra of the glasses were measured at room temperature in the wave number range from 200 to 1000 cm^{-1} using an Nd-YAG laser line at 1064 nm and a SPEX Triplemate 1877 Triple grating monochromator.

3. Results and discussion

The glass formation area of the CdO–WO_3–TeO_2 ternary system determined in the present study is given in Fig. 1. Compared with the reported glass forming regions by Imaoka and Yamazaki[24] and Safonov[25], the glass formation area was expanded under our experimental conditions. In our previous study,[9] the vitrification behavior of the tungsten–tellurite glasses were discussed and the glass formation range of the WO_3–TeO_2 binary system was reported as 4–35 WO_3 mol%.[9] The glass formation range of the CdO–TeO_2 binary system was reported in the literature by Mochida et al.[30] as 5–10 CdO mol%, however in our study on the phase equilibria of the CdO–TeO_2 system, the glass formation range of this system was expanded to 5–15 CdO mol% under our experimental conditions. In the present study, out of thirteen ternary samples prepared to determine the glass forming compositions of the CdO–WO_3–TeO_2 system, seven as-cast samples were obtained as glass (see Fig. 1). The obtained glass samples showed a color change from yellowish to pale orange with increasing WO_3 + CdO/TeO_2 ratio.

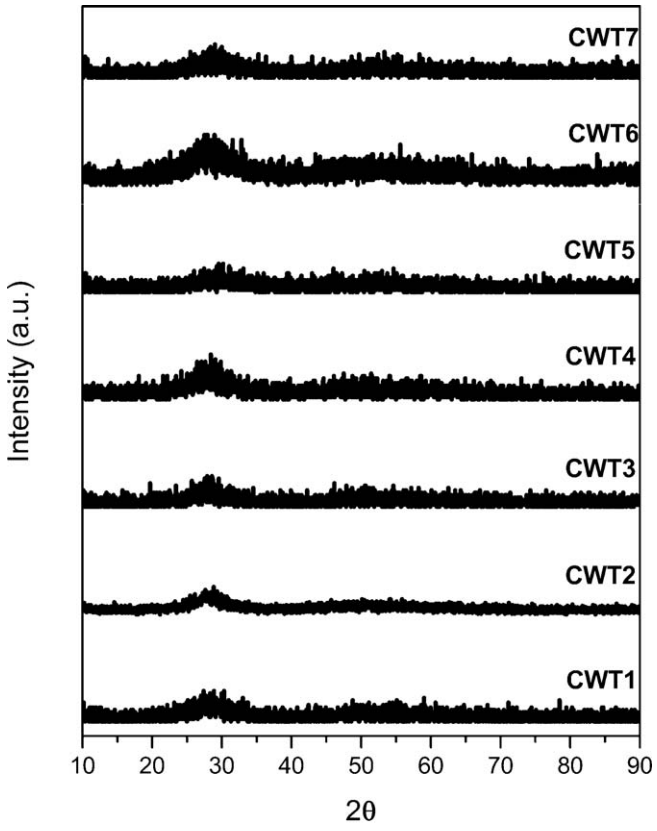

Fig. 2. X-ray diffraction patterns of the CdO–WO_3–TeO_2 glasses.

X-ray diffraction analyses were carried out to verify the glassy nature of the samples obtained as transparent bulk glasses and the results are shown in Fig. 2. XRD patterns of these samples revealed no detectable peaks, proving the vitreous structure. DSC analyses were carried out to determine the thermal behavior of the ternary CdO–WO_3–TeO_2 glasses. DSC thermograms are illustrated in the temperature range of 300–550 °C in Fig. 3 and the thermal analysis details are given in Table 1.

For all samples, a shallow broad endothermic change of the calorimetric signal corresponding to the glass transition, T_g, was observed between 319 and 387 °C. The glass transition temperatures shifted to higher values with the substitution of WO_3 and CdO for TeO_2, which was also reported in the literature for

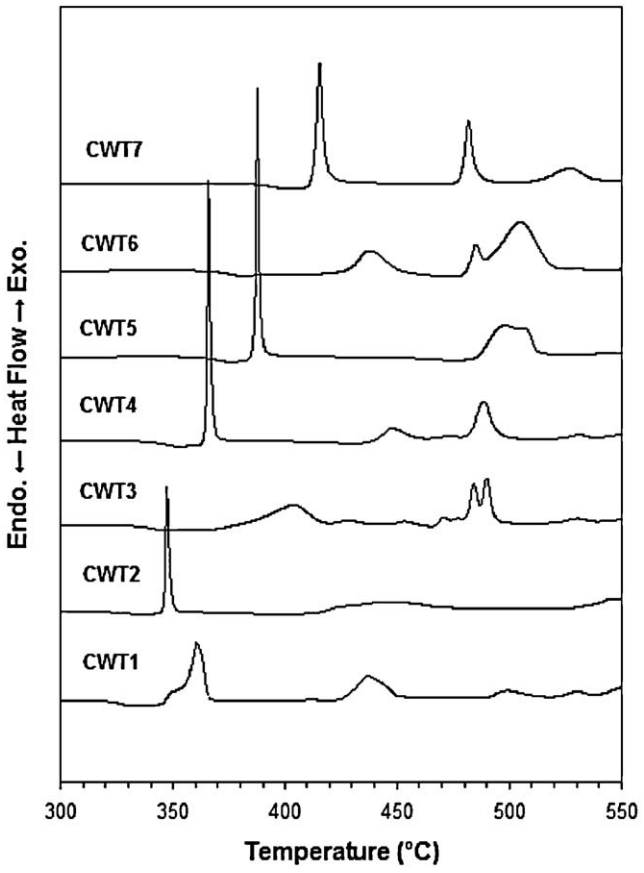

Fig. 3. DSC curves of the CdO–WO_3–TeO_2 glasses, scanned at a heating rate of 10 °C/min.

WO_3 and CdO containing binary tellurite glasses.[3,9,22] As can be seen in Fig. 3, different number of exothermic peaks, indicating crystallization reactions was observed with the change in composition. The crystallization onset and peak temperature values for the first exothermic reaction are given in Table 1. The temperature difference between T_g and the first exothermic peak onset T_c, ΔT, indicating a measure of the thermal stability against crystallization was calculated for all glass samples and listed in Table 1. The maximum ΔT value was found as 63 °C for CWT6 sample. The ΔT values obtained in the present study for CdO–WO_3–TeO_2 glasses were found to be lower than the glass stability values reported in the literature for tungsten–tellurite based binary and ternary glasses.[3,9,16,17,19] In general, the reason for low glass stability values was due to the crystallization of the δ-TeO_2 phase at lower temperatures. For CWT3 and CWT6 samples, which have lower CdO/WO_3 ratio than the other samples, the crystallization of the δ-TeO_2 phase was not observed; therefore higher ΔT values were calculated for those samples. This behavior can be explained as we reported in our previous study that the addition of CdO into tellurite glasses promotes the formation of δ-TeO_2 phase which lowers the ΔT values of the glasses.[6]

The activation enthalpy for glass transition, ΔH^*, and the fragility parameter, m, values which are often used to determine the strong–fragile characters of glass forming liquids[26,27] are given in Table 1. The activation enthalpy for glass transition was calculated by running DSC scans of glass samples at four different heating rates and ΔH^* values of the ternary glasses were found between 505 and 815 kJ/mol. The fragility parameters, m, which were calculated by using the ΔH^* values showed a decrease from 163 to 131 with the decreasing TeO_2 content. It was reported by Zhu et al.[26] that there is no sharp limit to characterize strong–fragile characters of liquids on the basis of fragility parameters. However, it was mentioned that a fragility value less than 90 can be attributed for strong liquids, whereas a value greater than 135 is typical for fragile liquids. Fragile liquids show a fast increase in their viscosity and a large change in their heat capacity as the glass transition temperature is approached; while the viscosity and heat capacity of strong liquids show a small change in the glass transition region.[26,27,31] Comparing the fragility values obtained in the present study with the values reported by Zhu et al.[26], it can be concluded that the CdO–WO_3–TeO_2 melts have a fragile character.

The measured density of the glass samples (ρ), the molar volume (V_M), and oxygen molar volume (V_O) values for the CdO–WO_3–TeO_2 glasses are listed in Table 1. The density values determined at room temperature showed a regular increase from 5.82 to 6.22 g/cm^3 with the decreasing TeO_2 content.

As seen in Table 1, the highest molar volume, V_M, corresponds to the CWT6 glass sample, which has the highest percentage of oxygen atoms. The molar volume of glasses, V_M, was found to increase with the substitution of TeO_2 by WO_3 for constant CdO content. This behavior can be explained due to the increase in the number of oxygen atoms in the ratio 3/2, which was also reported in the literature for WO_3–GeO_2–TeO_2 and PbO–WO_3–TeO_2 ternary glass systems.[17,27] Similarly, increasing the CdO/TeO_2 ratio for constant WO_3 content decreased the molar volume of the glasses.

In the present study, oxygen molar volume was observed to decrease with the substitution of TeO_2 by WO_3 for constant CdO containing glasses as the glass structure becomes denser. This was resulted due to the formation of more Te–O–W and W–O–W linkages and fewer Te–O–Te linkages with increasing WO_3 content, where higher field intensity of W^{6+} ions with respect to the field intensity of Te^{4+} ions yields a more compact packing of the glassy structure network.[29] However, for constant WO_3 content, V_O was found to increase with increasing CdO content.

Refractive indices, n, of the glasses at a wavelength of 632 nm are listed in Table 1. The obtained n values showed an increase from 2.03 to 2.21 with decreasing TeO_2 content. This behavior was observed due to the addition of WO_3 (2.68 Å^3) and CdO (2.91 Å^3) cations which have higher polarizability values compared to TeO_2 cation (2.44 Å^3).[32,33]

The structure of CdO–WO_3–TeO_2 glasses was studied extensively by using Raman scattering technique. CWT1, CWT4 and CWT5 glasses were selected to represent the shifts in Raman peak intensities and frequencies according to the decreasing TeO_2 content. Fig. 4 shows the Raman spectra of ternary glasses in the spectral range of 200–1000 cm^{-1} and the vibrational properties of ternary glasses are summarized in Table 2. Raman spectra of ternary glass samples showed broad peaks and shoulders and the broadening of peaks are attributed to the

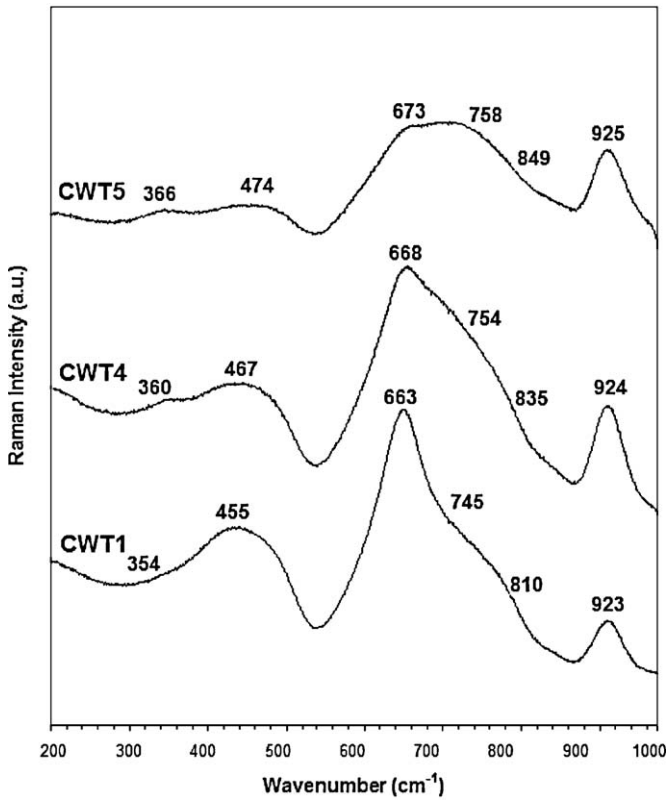

Fig. 4. Raman scattering spectra of the CWT1, CWT4, and CWT5 glasses.

disorderness. As seen in Fig. 4, the Raman spectra are dominated by a broad peak at around 663 cm^{-1} with a shoulder at around 745 cm^{-1} and the peaks slightly shifted and broadened with the decreasing TeO_2 content. Seven Raman peaks at around 205, 354, 455, 663, 745, 810 and 923 cm^{-1} were detected for these glasses. To find out the exact mode of vibrations, the Raman spectrum was deconvoluted into seven symmetrical Gaussian functions, by taking into account the Raman scattering spectra assignments for different tellurite based glasses reported in the literature.[17,20,34,35] Deconvoluted Raman spectra of CdO–WO_3–TeO_2 glasses are given in Fig. 5 and the Raman peaks are designated here as peaks *A*, *B*, *C*, *D*, *E*, *F* and *G*, respectively.

Table 2
Vibrational properties of CdO–WO_3–TeO_2 glasses.

Peak	Raman band (cm^{-1})	Vibrational mode
A	~205	Unidentified
B	352–372	Stretching vibrations of W–O–W in the WO_6 units
C	460–480	Stretching vibrations of Te–O–Te linkages
D	651–672	Stretching vibrations of TeO_4 tbp units
E	743–779	Stretching vibrations of TeO_3/TeO_{3+1} units
F	798–853	Stretching vibrations of W–O–W in WO_4 or WO_6 units
G	921–924	Stretching vibrations of W–O^- and W=O bonds inWO_4 or WO_6 units

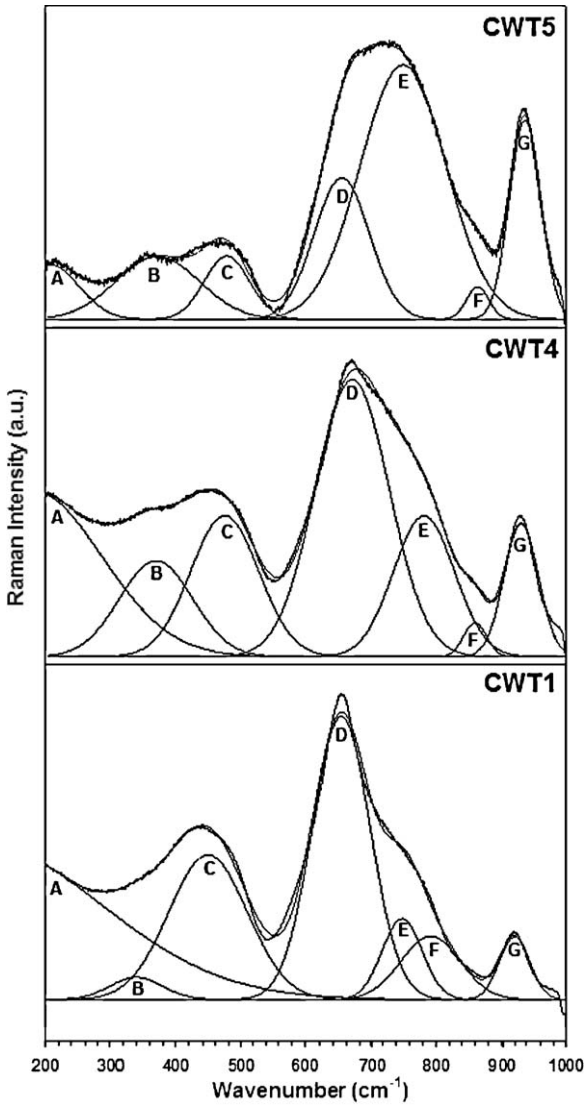

Fig. 5. The deconvolution of the Raman spectra of the CWT1, CWT4, and CWT5 glasses.

In Fig. 5, the peak A at around 205 cm^{-1}, observed in the Raman spectrum for the CdO–WO_3–TeO_2 glasses is attributed in the literature to the heavy metal vibrational modes by Tatar et al. for CdF_2–WO_3–TeO_2 glasses.[35] Upender et al. reported for WO_3–GeO_2–TeO_2 glasses that this peak might be assigned as a boson peak associated to light scattering due to acoustic-like vibrations of the disordered structure.[17] However, the origin of this peak remained not fully clear. The peak B at around 354–366 cm^{-1} belongs to the stretching vibrations of W–O–W in the WO_6 units. The peak C at around 455–474 cm^{-1} corresponds to the stretching vibrations of Te–O–Te linkages in between two TeO_4 four-coordinate atoms. The peak D at around 663–673 cm^{-1} is attributed to the Te–O stretching vibration of TeO_4 trigonal bipyramid (tbp) units corresponding to the strong Raman band of crystalline α-TeO_2. The peak E at around 745–758 cm^{-1} is due to $[TeO_{3+1}]^{4-}$, $[TeO_3]^{2-}$ units. The Raman peak F at around 810–849 cm^{-1} corresponds to the stretching vibrations of W–O–W in WO_4 or WO_6 units. Finally,

the peak G at around 923–925 cm^{-1} is assigned to the stretching vibrations of W–O^- and W=O bonds associated with WO_4 and WO_6 units, respectively, which was also observed for the binary WO_3–TeO_2 glasses.

Equimolar substitution of TeO_2 by WO_3 and CdO changed the intensities and positions of the Raman peaks. The increasing amount of WO_3 and CdO in CdO–WO_3–TeO_2 glasses resulted in a decrease in the intensities of peaks C and D which correspond to the stretching vibrations of Te–O–Te linkages and TeO_4 tbp units in the glass network, respectively. This was resulted due to the formation of more Te–O–W linkages and fewer Te–O–Te linkages with the increasing WO_3 content. The intensity change of peak E which is due to the presence of TeO_3 units in the glass network increased with the increasing WO_3 content. This behavior can be explained due to the transformation of TeO_4 units into TeO_3 units as the WO_3 content reaches to 20 mol%. The intensity of peak F decreased and the peak shifted to higher frequencies with decreasing TeO_2 content. The intensities of peaks B (354 cm^{-1}) and G (921 cm^{-1}) increased with increasing WO_3 content. As the WO_3 content increased, a shift in the Raman peaks B and G toward higher frequencies was observed. The observed shift in the Raman peak G toward higher frequencies and increase in the intensity of the peaks is an indication of the transformation of WO_4 units toWO_6 units. From all Raman spectra analyses, it can be concluded that the equimolar substitution of TeO_2 by WO_3 and CdO gives rise to structural transition in TeO_2 network due to the formation of non-bridging oxygens in the form of W–O^-, W=O, Te–O^- and Te=O bonds and the incorporation of Cd^{2+} ions does not originate new Raman bands.

4. Conclusion

The glass formation range of the CdO–WO_3–TeO_2 ternary system was investigated through DSC and XRD methods. The glass forming region was expanded comparing with the existing range reported in the literature. The obtained glass samples exhibited a color change from yellowish to pale orange with increasing WO_3 + CdO/TeO_2 ratio. DSC analyses showed that the glass transition temperatures shifted to higher values with the substitution of WO_3 and CdO by TeO_2. The maximum glass stability value, ΔT, was found as 63 °C for CWT6 sample. CdO–WO_3–TeO_2 glasses showed a fragile character with the calculated fragility parameters in the range of 163 and 131. The measured density values increased from 5.82 to 6.22 g/cm^3 with decreasing TeO_2 content. The molar volume of glasses was found to increase with the increase in number of oxygen atoms. The oxygen molar volume was observed to decrease as the glass structure becomes denser. Refractive indices at a wavelength of 632 nm showed an increase from 2.03 to 2.21 with decreasing TeO_2 content due to the addition of cations with higher polarizability. The Raman results showed that the equimolar substitution of TeO_2 by WO_3 and CdO results in continuous structural transition of TeO_4 units to TeO_3 units via TeO_{3+1} units and the increasing WO_3 content lead the formation of W–O–W and Te–O–W linkages, while that of Te–O–Te linkages decreased.

Acknowledgements

The authors of this study gratefully acknowledge The Scientific & Technological Research Council of Turkey (TUBITAK) for the financial support under the project numbered 108M077. Refractive index and Raman spectra measurements were carried out in part in the Frederick Seitz Materials Research Laboratory Central Facilities, University of Illinois.

References

1. El-Mallawany RAH. Tellurite glasses handbook. Boca Raton/London/New York/Washington, DC: CRC Press; 2002.
2. Blanchandin S, Marchet P, Thomas P, Champarnaud-Mesjard JC, Frit B, Chagraoui A. New investigations within the TeO_2–WO_3 system: phase equilibrium diagram and glass crystallization. *Journal of Materials Science* 1999;**34**:4285–92.
3. Kosuge T, Benino Y, Dimitrov V, Sato R, Komatsu T. Thermal stability and heat capacity changes at the glass transition in K_2O–WO_3–TeO_2 glasses. *Journal of Non-Crystalline Solids* 1998;**242**:154–64.
4. Shaltout I, Tang Y, Braunstein R, Abu-Elazm AM. Structural studies of tungstate–tellurite glasses by Raman spectroscopy and differential scanning calorimetry. *Journal of Physical Chemical Solids* 1994;**56**:141–50.
5. Öveçoğlu ML, Özen G, Cenk S. Microstructural characterization and crystallization behavior of $(1-x)TeO_2$–xWO_3 (x = 0.15, 0.25, 0.3 mol) glasses. *Journal of the European Ceramic Society* 2006;**26**:1149–58.
6. Ersundu AE, Karaduman G, Çelikbilek M, Solak N, Aydin S. Stability of the δ-TeO_2 phase in the binary and ternary TeO_2 glasses. *Journal of the European Ceramic Society* 2010;**30**:3087–92.
7. Ersundu AE, Karaduman G, Çelikbilek M, Solak N, Aydin S. Effect of rare-earth dopants on the thermal behavior of tungsten–tellurite glasses. *Journal of Alloys and Compounds* 2010;**508**:266–72.
8. Çelikbilek M, Ersundu AE, Solak N, Aydin S. Crystallization kinetics of the tungsten–tellurite glasses. *Journal of Non-Crystalline Solids* 2011;**357**:88–95.
9. Çelikbilek M, Ersundu AE, Solak N, Aydin S. Investigation on thermal and microstructural characterization of the TeO_2–WO_3 system. *Journal of Alloys and Compounds* 2011;**509**:5646–54.
10. Charton P, Gengembre L, Armand P. TeO_2–WO_3 glasses: infrared, XPS and XANES structural characterizations. *Journal of Solid State Chemistry* 2002;**168**:175–83.
11. Lezal D, Pedlikova J, Kostka P, Bludska J, Poulain M, Zavadil J. Heavy metal oxide glasses: preparation and physical properties. *Journal of Non-Crystalline Solids* 2001;**284**:288–95.
12. Intyushin EB, Novikov VA. Tungsten–tellurite glasses and thin films doped with rare-earth elements produced by radio frequency magnetron deposition. *Thin Solid Films* 2008;**516**:4194–200.
13. Mirgorodsky AP, Merle-Mejean T, Champarnaud JC, Thomas P, Frit B. Dynamics and structure of TeO_2 polymorphs: model treatment of paratellurite and tellurite; Raman scattering evidence for new δ- and γ-phases. *Journal of Physics and Chemistry of Solids* 2000;**61**:501–9.
14. Champarnaud-Mesjard JC, Blanchandin S, Thomas P, Mirgorodsky A, Merle-Mejean T, Frit B. Crystal structure, Raman spectrum and lattice dynamics of a new metastable form of tellurium dioxide: γ-TeO_2. *Journal of Physics and Chemistry of Solids* 1999;**61**:1499–507.
15. Sokolov VO, Plotnichenko VG, Dianov EM. Structure of WO_3–TeO_2 glasses. *Inorganic Materials* 2006;**43**:194–213.
16. Upender G, Ramesh S, Prasad M, Sathe VG, Mouli VC. Optical band gap, glass transition temperature and structural studies of $(100-2x)TeO_2$–xAg_2O–xWO_3 glass system. *Journal of Alloys and Compounds* 2010;**504**:468–74.
17. Upender G, Vardhani CP, Suresh S, Awasthi AM, Mouli VC. Structure, physical and thermal properties of WO_3–GeO_2–TeO_2 glasses. *Materials Chemistry and Physics* 2010;**121**:335–41.

18. Upender G, Sathe VG, Mouli VC. Raman spectroscopic characterization of tellurite glasses containing heavy metal oxides. *Physica B* 2010;**405**:1269–73.
19. Upender G, Bharadwaj S, Awasthi AM, Mouli VC. Glass transition temperature-structural studies of tungstate tellurite glasses. *Materials Chemistry and Physics* 2009;**118**:298–302.
20. Komatsu T, Mohri H. Raman scattering spectra and optical properties of tellurite glasses and crystalline phases containing PbO and CdO. *Physics and Chemistry of Glasses* 1999;**40**:257–63.
21. Kozhukharov V, Marinov M, Grigorova G. Glass-formation range in binary tellurite systems containing transition metal oxides. *Journal of Non-Crystalline Solids* 1978;**28**:429–30.
22. Zayas ME, Arizpe H, Castillo SJ, Medrano F, Diaz GC, Rincon JM, et al. Glass formation area and structure of glassy materials obtained from ZnO–CdO–TeO_2 ternary system. *Physics and Chemistry of Glasses* 2005;**46**:46–50.
23. Safonov VV, Tsygankov VN. Electrical properties of glasses in the systems BaO (Bi_2O_3, CdO, PbO)–TeO_2–WO_3 and CdO–PbO–TeO_2. *Inorganic Materials* 1996;**32**:984–7.
24. Imaoka M, Yamazaki T. Studies of the glass formation ranges of tellurite systems. *Journal of the Ceramic Society of Japan* 1968;**75**:160–72.
25. Safonov VV. The BaO(CdO)–TeO_2–WO_3 systems in the TeO_2 rich regions. *Zhurnal Neorganicheskoi Khimii* 1996;**41**:698–701.
26. Zhu D, Ray CS, Zhou W, Day DE. Glass transition and fragility of Na_2O–TeO_2 glasses. *Journal of Non-Crystalline Solids* 2003;**319**:247–56.
27. Brüning R, Sutton M. Fragility of glass-forming systems and the width of the glass transition. *Journal of Non-Crystalline Solids* 1996;**205**(207):480–4.
28. Moynihan CT. Correlation between the width of the glass transition region and the temperature dependence of the viscosity of high-T_g glasses. *Journal of American Ceramic Society* 1993;**76**:1081–7.
29. Munoz-Martín D, Villegas MA, Gonzalo J, Fernández-Navarro JM. Characterisation of glasses in the TeO_2–WO_3–PbO system. *Journal of the European Ceramic Society* 2009;**29**:2903–13.
30. Mochida N, Takahshi K, Nakata K, editors. Journal of the Ceramic Society of Japan 1978; 86:317, quoted by El-Mallawany RAH. Tellurite glasses handbook. Boca Raton/London/New York/Washington, DC: CRC Press; 2002.
31. Voivod IS, Poole PH. Sciortino fragile-to-strong transition and polyamorphism in the energy landscape of liquid silica. *Nature* 2001;**412**: 514–7.
32. Vithal M, Nachimuthu P, Banu T, Jagannathana R. Optical and electrical properties of PbO–TiO_2, PbO–TeO_2, and PbO–CdO glass systems. *Journal of Applied Physics* 1997;**81**:7922–6.
33. O'Deonnell MD, Richardson K, Stolen R, Seddon AB, Furniss D, Tikhomirov VK, et al. Tellurite and fluorotellurite glasses for fiberoptic Raman amplifiers: glass characterization, optical properties, Raman gain, preliminary fiberization, and fiber characterization. *Journal of American Ceramic Society* 2007;**90**:1448–57.
34. Chowdari BVR, Kumari PP. Structure and ionic conduction in the Ag_2O–WO_3–TeO_2 glass system. *Journal of Material Science* 1998;**33**:3591–9.
35. Tatar D, Özen G, Erim FB, Öveçoğlu ML. Raman characterizations and structural properties of the binary TeO_2–WO_3, TeO_2–CdF_2 and ternary TeO_2–CdF_2–WO_3 glasses. *Journal of Raman Spectroscopy* 2010;**41**:797–807.